Bull. Astr. Soc. India (2001) **29**, 53–7

A study of the old galactic star cluster Berkeley 32

T. Richtler[1] and Ram Sagar [2,3]

[1] *Departamento de Física, Universidad de Concepción, Casilla 160-C, Concepción, Chile*
[2] *State Observatory, Manora Peak, Naini Tal 263129, Uttaranchal, India*
[3] *Sternwarte der Universität Bonn, Auf dem Hügel 71, D-53121 Bonn, Germany*

Received 13 September 2000; accepted 9 January 2001

Abstract. We present new CCD photometry of the distant old open star cluster Berkeley 32 in Johnson V and Cousins I passbands. A total of ~ 3200 stars have been observed in a field of about 13′ x 13′. The colour-magnitude diagram (CMD) in V, $(V-I)$ has been generated down to V = 22 mag. A broad but well defined main sequence is clearly visible. Some blue stragglers, a well developed subgiant branch and a Red Clump are also seen. By fitting isochrones to this CMD as well as to other CMDs available in the literature, and using the Red Clump location, the reddening, distance and age of the star cluster have been determined. The cluster has a distance of ~ 3.3 kpc, its radius is about 2.4 pc; the reddening E(B-V) is 0.08 mag and the age is ~ 6.3 Gyr. By comparison with theoretical isochrones, a metallicity of [Fe/H] ≈ –0.2 dex has been estimated.

Theoretical isochrones have been used to convert the observed cluster luminosity function into a mass function in the mass range ~ 0.6–1.1 $M_{\odot}$. We find a much flatter mass function than what has been found for young clusters. If the mass function is a power law $dN \sim m^{\alpha}dm$, then we get $\alpha = -0.5 \pm 0.3$. This may be seen as a signature of the highly evolved dynamical state of the cluster.

Key words : Open star clusters: individual: Berkeley 32 - star: evolution - HR diagram - Mass functions - Galactic disk.

1. Introduction

Berkeley 32 (*C*0655+065 ~ OCL 522, l=207.°95, b=4.°4), also known as Biurakan 8, is a small galactic (open) star cluster of angular diameter ~ 6′. It is located in the Galactic anticentre direction and has been classified as Trumpler class II2m (Lyngå 1987). This object was discovered by Iskudarjan (1960) and catalogued by Setteducati & Weaver (1960). On the sky survey maps, the cluster appears to be rich and likely of old age (cf. King 1964). The first photometric study

of the cluster was carried out by Kaluzny & Mazur (1991) in the *UBV* and Washington systems by CCD imaging of an area ~ 6.′6 x 6.′6. They presented the colour-magnitude diagram (CMD) and discussed its morphology, derived cluster reddening and distance as $E(B–V)$ = 0.16 mag and 3.1±0.2 kpc respectively, and estimated the metallicity as [Fe/H] = –0.37 ± 0.05. They derived an age of ~ 6 Gyr. Using morphological age parameters, Janes & Phelps (1994) estimated an age of 7.2 Gyr for Berkeley 32.

Scott et al. (1995) have determined radial velocities of 7 cluster members and found a mean heliocentric radial velocity of + 101±3 km/sec, which among their cluster sample deviates most from a pure Galactic rotation after Berkeley 17.

Mass function studies of open star clusters indicated that the slopes of the mass functions of older (age > 1 Gyr) clusters differ significantly from each other and also are not uniform over the entire mass range (cf. Sagar & Griffiths 1998b). However, the number of old objects studied so far is small. As such, a study of the old cluster Berkeley 32 can contribute interesting knowledge on the mass function of old, probably highly evolved clusters.

Our aim is to re-analyse Berkeley 32 with deeper photometry than Kaluzny & Mazur (1991) had at their disposal and study its mass function which is lacking. The observations, data reductions and comparison with earlier photometry are given in the next two sections. The cluster radius, other photometric results and mass function of the cluster are described in the subsequent sections of the paper.

2. Observations and Reductions

The CCD observations have been obtained on 1999 March 22 with the 3.5m telescope at Calar Alto Observatory, Spain, run by the Max-Planck Institute for astronomy, Heidelberg. The focal reducer MOSCA attached at the RC Cassegrain focus provided an effective f/2.7 focal ratio (**http://www.caha.es/caha/instruments/mosca/manual.html**). The observations have been carried out in the Johnson *V* and Cousins *I* filters using the SITE 18b CCD chip. Each pixel (24μ square) corresponded to 0.″53 x 0.″53 on the sky. The non-vignetted area of the CCD was 1500 x 1500 pixel^2 providing a field of about 13.′25 x 13.′25. The read-out noise was 5.4 electrons per pixel and the ratio electrons-per-ADU was ~ 2.7. Figure 1 shows the finding chart for the imaged cluster region and Table 1 lists the log of the observations. For calibration purpose, we observed the standard star field SA 98 (Landolt 1992).

The present observations were carried out as a back-up programme. We therefore could not observe standard stars during the whole night. Instead, we observed the standard field SA 98 three times: before, between, and after the observations of Berkeley 32 (Table 1). The strategy was to observe Berkeley 32 at a similar air-mass as the standard fields, so that one can calibrate photometric data of the cluster region with an accuracy of a few percent without a precise determination of the atmospheric extinction coefficients. The basic processing of the data frames was done in the standard manner using the MIDAS data reduction package. The uniformity of flat fields is better than one percent in both filters.

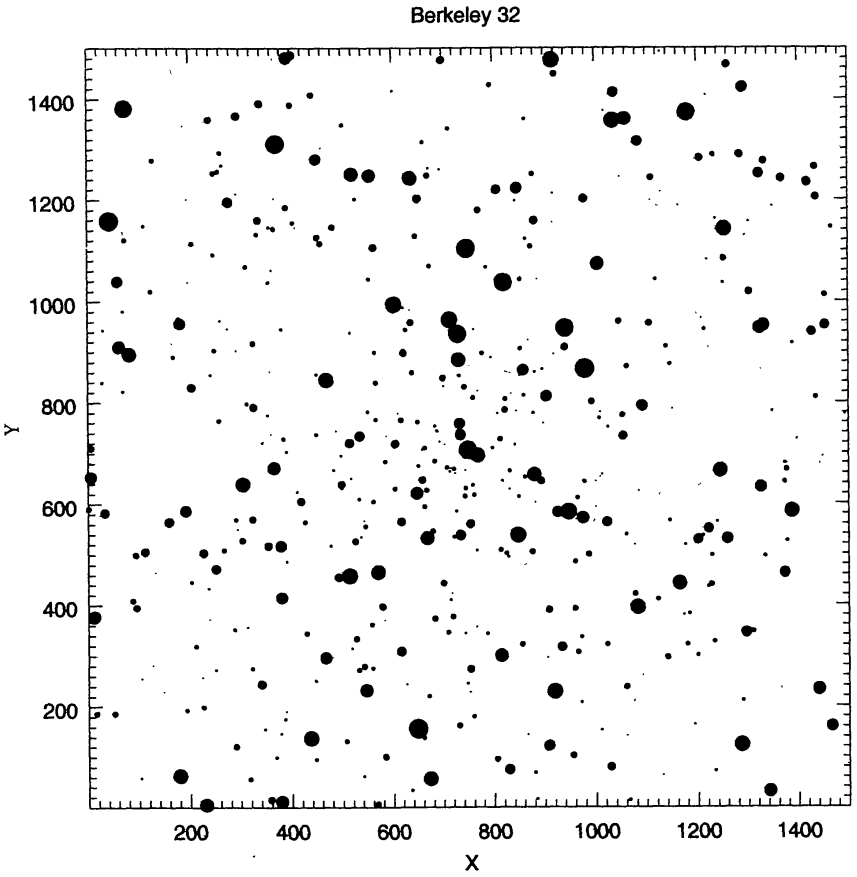

Figure 1. Identification chart for the Berkeley 32 region. The (X,Y) coordinates are in CCD pixel units and one CCD pixel corresponds to 0.″53 on the sky. North is up and East to the left. Filled circles of different sizes represent the brightness of the stars. The smallest size denotes stars of V = 17 mag.

Instrumental magnitudes have been measured using the DAOPHOT software (Stetson 1987, 1992) under MIDAS. The image parameters and errors provided by DAOPHOT were used to reject poor measurements. About 10% of the stars were rejected in this process. In those cases where brighter stars are saturated on deep exposure frames, their magnitudes have been taken only from the short exposure frames. Most of the stars brighter than V ~ 12 mag could not be measured because they were saturated even on the shortest exposure frames. The CCD instrumental magnitudes have been calibrated using the observations of the SA 98 field and the following relations

$$V - v = a0 + a1 * (V - I); \qquad (V - I) - (v - i) = b0 + b1 * (V - I)$$

where capital letters denote standard magnitudes and colours, and lower case letters denote instrumental values. The values refer to exposure time of 1 second. These equations along with the site mean atmospheric extinction values of 0.15±0.04 and 0.09±0.02 mag per unit air-mass in V and $(V - I)$ respectively were used in determining the colour equations for the system as well as the zero-points. The effects of uncertainties in atmospheric extinction values are

maximum on zero-points but least on the colour coefficients. We therefore averaged the colour coefficients from the individual standard observations. With these values fixed we calculated the zero-points. Table 2 lists the colour coefficients and zero-points derived in this way. The

Table 1. Log of CCD observations of the cluster Berkeley 32 and the calibration region SA 98 (Landolt 1992). The data have been obtained on March 22, 1999.

Object	Time (UT)	Filter	Exposure time (seconds)	Air-mass
SA 98	19:23:45	*V*	8	1.27
SA 98	19:29:00	*I*	8	1.27
Be 32	19:40:04	*V*	10	1.17
Be 32	19:44:57	*V*	60	1.18
Be 32	19:49:05	*I*	8	1.18
Be 32	19:51:47	*I*	40	1.18
Be 32	19:54:36	*I*	3	1.19
SA 98	20:00:04	*V*	10	1.30
SA 98	20:02:37	*I*	8	1.30
Be 32	20:05:29	*V*	10	1.20
Be 32	20:07:44	*V*	100	1.20
Be 32	20:11:37	*I*	8	1.21
Be 32	20:14:04	*I*	80	1.21
SA 98	20:43:19	*V*	10	1.39
SA 98	20:45:37	*I*	8	1.40

Table 2. Colour coefficients and zero-points are for 1 second exposure time of the standard stars.

Air-mass	$a0 \pm \sigma$	$a1 \pm \sigma$	$b0 \pm \sigma$	$b1 \pm \sigma$
1.27	–0.513 ± 0.01	0.07 ± 0.01	0.667 ± 0.02	0.03 ± 0.003
1.30	–0.523 ± 0.02	0.07 ± 0.01	0.664 ± 0.02	0.03 ± 0.003
1.39	–0.573 ± 0.02	0.07 ± 0.01	0.643 ± 0.02	0.03 ± 0.003

Table 3. Internal photometric errors as a function of brightness. σ is the standard deviation in magnitude.

Mag range	σ_V	σ_I
12.0 – 14.0	0.005	0.010
14.0 – 16.0	0.005	0.010
16.0 – 17.0	0.005	0.010
17.0 – 18.0	0.006	0.013
18.0 – 19.0	0.009	0.024
19.0 – 20.0	0.017	0.051
20.0 – 21.0	0.041	0.117
21.0 – 22.0	0.106	
22.0 – 23.0	0.221	

zero-points are uncertain by ~ 0.02 mag in V and $(V - I)$. The internal errors as a function of magnitude for each filter are given in Table 3. The errors become large (> 0.15 mag) for stars fainter than V = 22 and I = 21 mag. The X and Y pixel coordinates as well as the V and $(V - I)$ magnitudes and DAOPHOT errors of the stars observed in Berkeley 32 are listed in Table 4. Stars observed by Kaluzny & Mazur (1991) have been identified in the last column. Table 4 is available only in electronic form at the open cluster database Web site at **http:// obswww.unige.ch/webda/**. It can also be obtained from the authors.

3. Comparison with previous photometry

In this section, we compare the present CCD photometry with the only previous CCD photometric observations of the cluster by Kaluzny & Mazur (1991) in the only common passband V. The transformation equations relating their (X_{km}, Y_{km}) coordinate system to ours (X_{pres}, Y_{pres}) were found to be

$$X_{pres} = 1178.252 - 0.024X_{km} - 1.512Y_{km}; \qquad Y_{pres} = 259.383 + 1.511X_{km} - 0.024Y_{km}$$

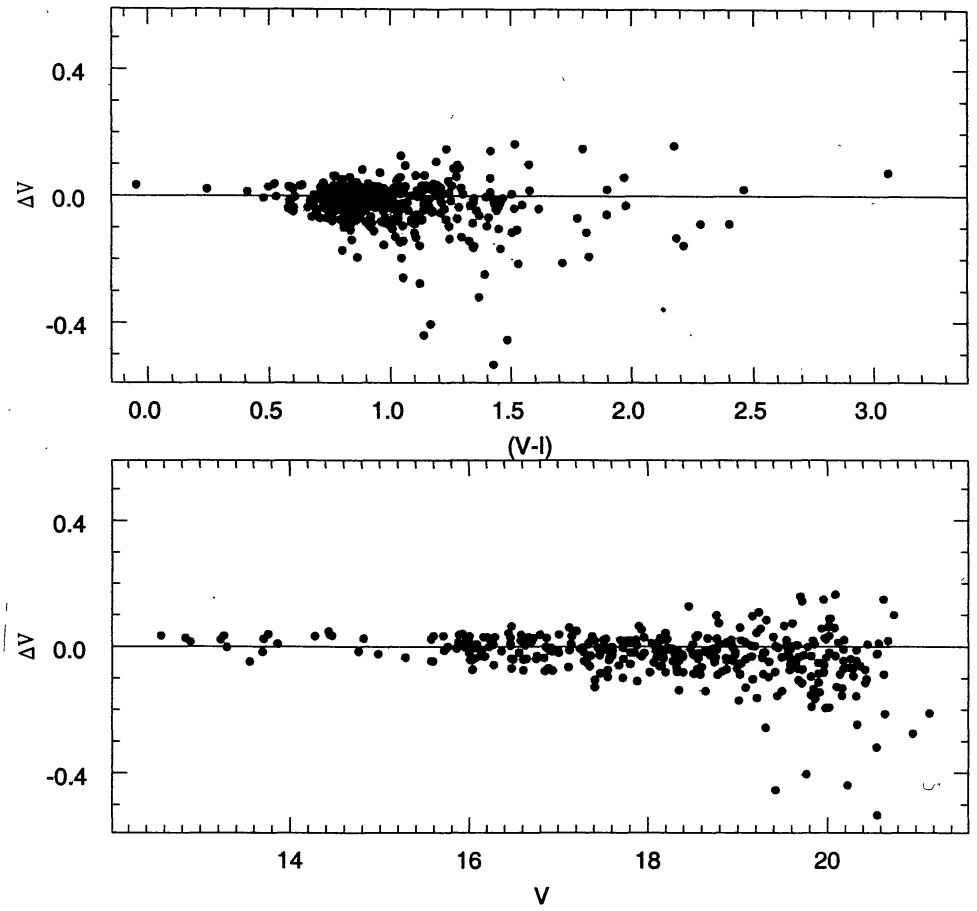

Figure 2. Comparison of the present V magnitude with those of Kaluzny & Mazur (1991). The differences (△) are in the sense of this study minus Kaluzny & Mazur. They are plotted against the present CCD photometry.

There are 835 stars measured by Kaluzny & Mazur (1991) whose positions coincide within 1 pixel with the stars positions measured by us. The differences (ΔV) between the present data and data obtained by them are plotted in Fig. 2, while the statistical results are given in Table 5. These show that except for a few outliers, which appear to be mostly stars that were treated as single in one study and as double (due to blending) in the other, the distribution of the photometric differences seems fairly random with almost no zero-point offset. As expected, the scatter increases with decreasing brightness and becomes more than ~ 0.1 mag at fainter levels. Considering the uncertainties present in our and Kaluzny & Mazur's (1991) measurements, we conclude that they are in very good agreement.

Table 5. Statistical results of the photometric comparison with data from Kaluzny & Mazur (1991). The difference (Δ) is in the sense present minus comparison data. The mean and standard deviation (σ) are based on N stars. A few points discrepant by more than 3.5 σ have been excluded from the analysis.

V range (mag)	ΔV Mean±σ	N	$(V-I)$ range (mag)	ΔV Mean±σ	N
12 – 14	0.006±0.03	17	–0.1–0.65	–0.021±0.16	41
14 – 16	–0.012±0.04	67	0.65–0.8	–0.013±0.12	197
16 – 17	–0.004±0.04	129	0.8–1.0	–0.020±0.12	242
17 – 18	–0.015±0.08	144	1.0–1.5	–0.026±0.11	286
18 – 19	–0.029±0.09	159	1.5–3.2	–0.011±0.11	69
19 – 20	–0.015±0.14	157			
20 – 21	–0.023±0.16	162			

4. Radius of the cluster

We used radial stellar density profile for the determination of cluster radius. Such determinations can provide ambiguous results as it depends on the limiting magnitude of the star counts. The fainter the stars are, the larger becomes the cluster radius, if mass segregation due to two-body relaxation is present. Given these caveats, it is not our aim to derive a dynamically relevant radius, but to determine the region where the cluster population dominates over field stars so that it can be used for investigations of the cluster properties.

We derived the position of the cluster centre by iteratively calculating the average X and Y positions of stars within 150 pixels from an eye estimated centre, until it converged to a constant value. The (X,Y) pixel coordinates of the cluster centre are (700, 665) with an accuracy of few pixels. The radial stellar density profile determined up to ~ 6′ from the cluster centre using stars brighter than V=18 mag is plotted in Fig. 3. The radius at which the star density flattens is considered as cluster radius which is ~ 2.′7. This agrees fairly well with the value of 3′ given by Lyngå (1987). We fit the following form of a King (1962) profile to the observed stellar density distribution

$$f(r) \propto C.\left(\frac{1}{\sqrt{(1+(r/r_c)^2)}} - \frac{1}{\sqrt{(1+(r_t/r_c)^2)}}\right)^2,$$

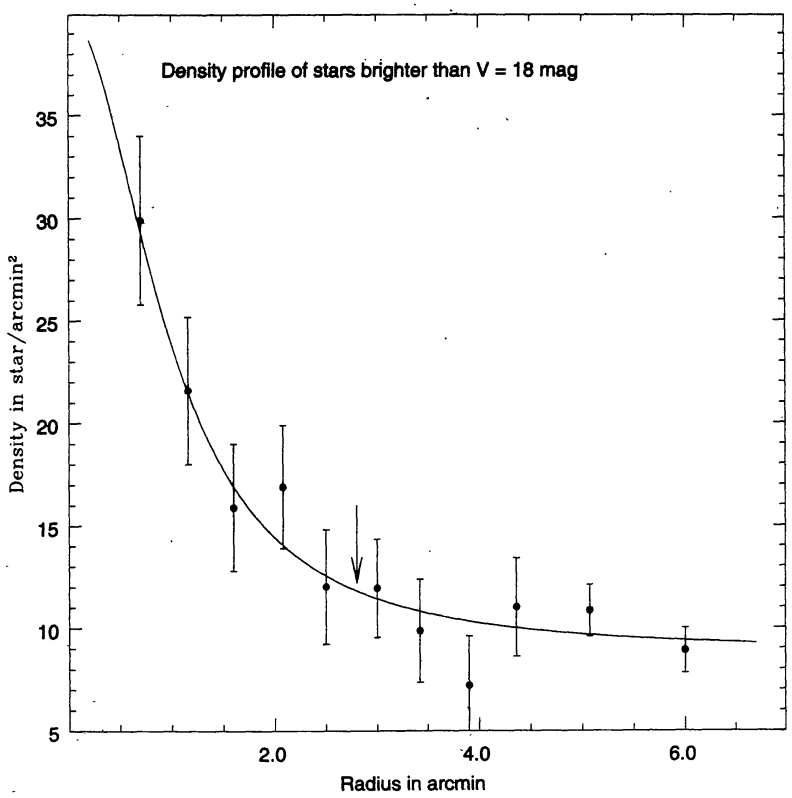

Figure 3. Plot of the radial density profile (•) for stars brighter than V = 18 mag in Berkeley 32 region. The length of the bar represents errors resulting from sampling statistics. Overplotted (solid curve) is a King (1962) profile with parameters given in the text. The arrow denotes the radius where the surface density of cluster stars becomes comparable with the field star density.

where C is the central stellar density, r_c and r_t are the core and tidal radius respectively. A least square fitting of the profile to the observed points yielded C = 33.9 ± 8 star/arcmin^2, r_c = 1.0 ± 0.38 arcmin and r_t = 23 ± 50 arcmin.

5. Colour-magnitude diagrams (CMDs)

5.1 The V, $(V-I)$ CMD

We plot the V, $(V-I)$ CMD for all (~ 3200) measured stars in the region of Berkeley 32 in Fig. 4(A). The CMD reaches down to V = 22 mag. The cluster main-sequence (MS) contaminated by field stars is clearly visible. Although it is clear that the stellar population of this region is of composite nature, the cluster population appears to be dominating. The only way to sharpen morphological features of the cluster sequence in the CMD is to select stars with small radial distances by compromising between a decreasing number of cluster stars and an increasing field population. The Fig. 4(B) shows our best result. Here we have selected only stars with a radial distance up to ~ 2.′7. The features of a very old open star cluster namely the distinct turn-off region and the subgiant branch are now very clearly visible. The giant branch (GB) is very sparsely populated and not well defined. Moreover, a group of stars can be seen which are brighter and bluer than the MS turn-off point suggesting that some of them are blue

stragglers (BSs). Such objects have been found in most intermediate and old age open star clusters (see Kaluzny 1994; Phelps et al. 1994; Sagar & Griffiths 1999a). Many of them have been identified as close binary systems. The (X,Y) pixel coordinates, radius, magnitudes and colour of the stars located in the GB, red GB and BS regions of the CMDs are given in Table 6. The cluster membership of these stars is also indicated in the table. A star is considered as probable cluster member if it lies within ± 0.05 mag in colour and ± 0.1 mag in brightness with respect to the isochrone of the cluster age at least in two of the V, $(U - V)$; V, $(B - V)$ and V, $(V - I)$ diagrams. In addition, brightening due to unresolved/optical binary stars has also been considered.

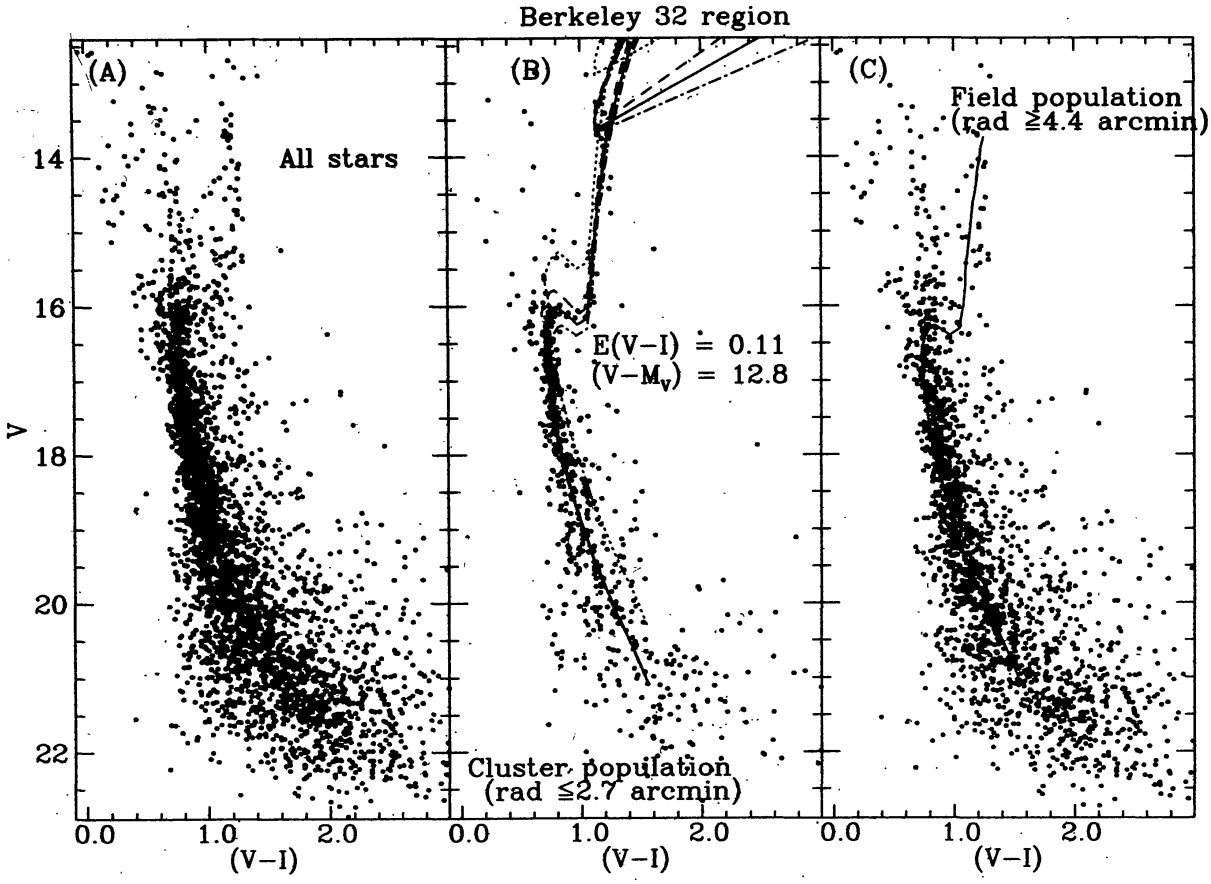

Figure 4. V, $(V - I)$ diagrams (A) for all stars observed by us, (B) for the cluster population (stars with radius ≤ 2.′7) and (C) for the field population (stars with radius ≥ 4.′4) in the Berkeley 32 region are plotted. The composite nature of the stellar population is apparent in (A). In the cluster population, the Bertelli et al. (1994) isochrones for z = 0.008 and log (age) = 9.7 (short-dashed), 9.8 (continuous) and 9.9 (dot-short dashed) are shown. The isochrone of log (age) = 9.8 found to be best fitting to the observed cluster sequence with a reddening of $E(V - I)$ = 0.11 (or $E(B - V)$ = 0.08) and an apparent distance modulus of 12.8 mag. The dotted curve shows the extent that binaries of equal mass can brighten the isochrone of log (age) = 9.8. In the field population, the overplotted curve is displaying the cluster locus. There are red giants resembling cluster giant branch stars. A considerable part of the main sequence population has a turn-off similar to the cluster. but the bulk of the main sequence stars are clearly shifted towards the red, indicating higher reddening, and thus a background stellar population.

Table 6. Spatial and *UBVI* photometric values of the candidate giant branch and blue straggler stars are listed along with the identification of Kaluzny & Mazur (1991) prefixed with KM. The $(U - B)$ and $(B - V)$ values are taken from Kaluzny & Mazur (1991). The probable photometric members have been identified as PM in the last column.

(A) Stars redder than MS turn-off (candidate for giant branch)

Star	X (pixel)	Y (pixel)	Radius (pixel)	V (mag)	$(U - B)$ (mag)	$(B - V)$ (mag)	$(V - I)$ (mag)	Other identification	Membership
226	813.65	509.20	192.85	16.00	0.18	0.64	0.74	KM86	PM
238	525.10	526.47	223.12	15.57	0.83	1.05	1.14	KM59	
242	667.64	532.82	136.08	13.86	0.85	1.10	1.19	KM21	PM
245	720.59	535.05	131.57	16.22	0.07	0.59	0.71	KM120	PM
254	679.15	546.71	120.11	15.87	0.62	0.97	1.10	KM74	PM
264	426.71	564.67	291.12	16.03	0.15	0.67	0.79	KM108	PM
269	975.20	571.96	290.50	14.28	0.88	1.14	1.25	KM24	PM
274	947.00	584.20	259.88	13.27	0.66	1.01	1.13	KM10	PM
293	760.87	617.50	77.21	16.08	0.11	0.62	0.74	KM103	PM
302	603.93	629.92	102.27	16.02	0.09	0.57	0.69	KM91	PM
310	498.03	639.10	203.62	15.28	0.80	1.01	1.06	KM46	PM
318	880.21	657.52	180.37	13.76	0.78	1.08	1.18	KM19	PM
331	584.61	683.34	116.84	16.14	0.30	0.77	0.88	KM113	PM
332	682.86	684.53	25.98	16.00	1.10	1.15	1.34	KM93	
347	748.92	706.51	64.16	12.90	0.68	1.02	1.06	KM8	
352	514.50	720.01	193.48	14.98	0.12	0.68	0.78	KM38	
357	812.84	727.41	128.95	15.88	0.63	0.96	1.04	KM75	PM
360	534.13	733.92	179.62	14.76	0.80	1.16	1.25	KM33	
414	759.17	809.22	155.89	16.01	0.19	0.69	0.82	KM87	PM
416	904.29	812.04	251.70	14.43	0.88	1.12	1.24	KM27	PM
419	859.71	813.91	218.36	16.29	0.11	0.60	0.72	KM131	PM
449	896.58	866.32	281.38	16.44	0.12	0.59	0.72	KM143	PM
456	730.79	884.57	221.72	13.71	0.79	1.07	1.14	KM17	PM
465	777.42	897.74	245.28	16.07	0.45	0.87	0.98	KM100	PM
488	625.73	944.14	288.85	16.14	0.40	0.83	0.88	KM116	PM
963	699.83	443.49	221.51	15.59	0.06	0.57	0.69	KM58	PM
974	570.29	464.89	238.47	13.70	0.77	1.05	1.15	KM18	PM
991	824.76	502.60	204.79	16.08	0.10	0.60	0.74	KM101	PM
1061	532.84	609.89	176.01	16.27	0.97	1.02	1.11	KM137	
1077	757.98	637.12	64.33	16.24	0.10	0.60	0.72	KM122	PM
1089	861.68	652.43	162.17	16.16	0.27	0.81	0.95	KM110	PM
1101	720.91	668.72	21.24	16.15	0.12	0.61	0.71	KM112	PM
1104	707.22	671.58	9.77	16.09	0.13	0.61	0.73	KM105	PM
1116	751.69	691.00	57.86	16.38	0.05	0.64	0.68	PM138	PM
1128	663.60	710.11	57.96	16.04	0.19	0.65	0.76	KM92	PM
1132	797.78	710.48	107.84	16.35	0.11	0.61	0.68	KM136	PM
1147	448.68	737.15	261.47	16.21	0.14	0.63	0.77	KM128	PM
1158	649.41	762.07	109.46	16.10	0.33	0.71	0.82	KM117	PM
1171	878.02	779.25	211.53	16.37	1.19	1.46	1.99	KM140	
1179	821.92	785.28	171.27	15.64	0.10	0.59	0.70	KM57	PM
1626	682.58	373.01	292.51	15.70	0.61	1.00	1.09	KM61	PM
1640	828.25	495.86	212.26	16.44	0.09	0.59	0.77	KM149	PM
1642	875.89	505.16	237.67	15.68	0.59	0.98	1.09	KM62	PM
1650	753.47	560.60	117.30	15.08	0.17	0.65	0.70	KM39	
1654	925.16	583.53	239.45	14.55	0.61	0.99	1.15	KM29	PM
1656	725.49	585.68	83.32	16.40	0.07	0.61	0.71	KM146	PM
1657	662.72	594.85	79.44	15.98	0.18	0.73	0.83	KM88	PM

Table 6. Continued.

Star	X (pixel)	Y (pixel)	Radius (pixel)	V (mag)	$(U-B)$ (mag)	$(B-V)$ (mag)	$(V-I)$ (mag)	Other identification	Membership
1661	561.13	604.88	151.33	16.06	0.42	0.87	0.98	KM97	PM
1662	418.84	605.15	287.46	15.24	1.58	1.50	1.61	KM47	
1663	964.84	611.62	270.17	16.10	0.24	0.78	0.89	KM98	PM
1666	666.79	627.02	50.45	15.95	0.07	0.62	0.69	KM84	PM
1668	393.35	645.43	194.34	15.35	0.33	0.71	0.80	KM45	PM
1675	831.23	665.10	131.23	16.22	0.06	0.61	0.71	KM119	PM
1685	768.41	695.85	75.04	13.64	0.72	1.06	1.15	KM16	PM
1691	604.59	718.30	109.29	15.15	0.32	0.82	0.95	KM41	
1701	566.32	766.05	167.58	16.17	.0.10	0.61	0.72	KM118	PM
1702	616.26	765.31	130.67	15.80	0.62	0.97	1.07	KM71	PM
1714	741.70	830.99	171.15	15.82	0.12	0.60	0.71	KM69	PM
1717	566.13	838.96	219.51	15.96	0.88	1.01	1.11	KM90	PM
1718	732.24	853.39	191.13	16.27	0.14	0.60	0.75	KM126	PM
1895	578.41	396.63	294.63	15.46	0.58	0.86	0.89	KM52	PM
1937	477.11	518.17	266.91	16.43			0.71		PM
1948	847.47	538.41	194.35	13.42	0.83	1.11	1.21	KM12	PM
1986	498.72	632.23	203.93	16.35	0.34	0.76	0.82	KM141	
1996	977.95	643.70	278.76	16.15	0.53	1.08	1.04	KM127	PM
2009	482.78	667.41	217.23	16.44			0.72		PM
2034	687.78	743.96	79.90	16.38	0.19	0.66	0.74	KM145	PM
2239	658.40	647.67	45.07	15.36	0.65	0.99	1.07	KM50	PM
2247	733.91	736.48	79.12	14.51	0.46	0.89	0.98	KM32	
2260	853.02	906.84	286.18	16.14	0.28	0.72	0.79	KM104	PM
2307	492.18	455.51	295.09	15.14	0.35	0.72	0.76	KM42	
2313	853.66	539.06	198.68	16.14	0.10	0.62	0.76	KM114	PM

(B) Stars bluer than the MS turn-off (candidate for blue straggler)

Star	X (pixel)	Y (pixel)	Radius (pixel)	V (mag)	$(U-B)$ (mag)	$(B-V)$ (mag)	$(V-I)$ (mag)	Other identification	Membership
169	718.22	376.70	288.88	15.86	0.17	0.40	0.48	KM72	PM
292	742.54	615.41	65.34	15.97	0.16	0.39	0.41	KM82	PM
303	743.82	631.21	55.33	16.07	0.07	0.50	0.60	KM102	PM
373	684.03	753.60	90.03	16.36	0.09	0.54	0.58	KM144	PM
413	823.05	806.89	187.81	16.00	0.11	0.54	0.63	KM85	PM
433	468.83	844.78	292.85	13.55	0.08	0.54	0.60	KM14	
442	638.28	859.77	204.32	15.95	0.11	0.51	0.61	KM81	PM
446	858.62	863.88	254.39	14.44	0.12	0.46	0.52	KM26	
507	712.97	963.58	298.86	13.23	0.18	0.27	0.25	KM9	
1027	545.34	556.03	189.19	16.03	0.17	0.49	0.59	KM99	PM
1064	849.30	614.48	157.62	16.26	0.12	0.49	0.60	KM125	PM
1237	564.34	899.03	270.51	16.20	0.17	0.47	0.57	KM123	PM
1651	616.62	565.03	130.18	15.12	0.17	0.22	0.22	KM40	
1680	650.47	675.41	50.61	16.26	0.08	0.49	0.57	KM129	PM
1684	742.58	694.04	51.54	15.81	0.00	0.60	0.61	KM68	PM
1700	732.72	758.40	98.97	14.57	0.16	0.21	0.15	KM30	
1728	728.99	935.80	272.35	12.86	0.10	0.60	0.63	KM6	
1911	513.95	458.03	278.30	13.39	0.07	0.49	0.55	KM13	
1947	733.43	538.40	130.94	14.73	0.17	0.29	0.31	KM31	
2041	549.93	781.97	190.27	16.29	0.14	0.47	0.54	KM131	PM
2062	699.50	848.78	183.78	15.57	0.16	0.42	0.43	KM55	PM
2079	621.45	898.18	246.05	15.36	0.11	0.54	0.62	KM48	PM
2400	647.52	621.46	68.19	14.13	0.09	0.55	0.62	KM23	

Fig. 4(C) shows the V, $(V - I)$ diagram of stars with radial distances more than ~ 4.′4 from the cluster centre. Overplotted are the fiducial points of the cluster sequence. There are a few red giants, which perhaps still belong to the cluster. A considerable part of the main sequence population has a turn-off similar to the cluster, but the bulk of the main sequence stars are clearly shifted towards the red, indicating higher reddening, and thus a background population. However, the interesting question whether there are evaporated stars surrounding the cluster cannot be answered on the basis of the present data. For this, kinematic informations like proper motions and radial velocities of these stars are required.

5.2 The cluster age from the "Red Clump"

It is well known that for intermediate and old open star clusters, the location of the Red Clump (RC) (the more massive analog of the horizontal branch in globular clusters) relative to the MS turn-off point is correlated with age (cf. Kaluzny 1994; Phelps et al. 1994; Carraro & Chiosi 1994; Pandey et al. 1997 and references therein). The two morphological parameters generally used for estimating cluster ages are the differences in magnitudes (ΔV) and colours ($\Delta(B - V)$ or $\Delta\ (V - I)$ between the RG branch at the level of the clump and the MS turn-off point, with the advantage that no prior knowledge of cluster distance, reddening and accurate metallicity is required.

Following Kaluzny (1994), we find $\Delta V = 2.7 \pm 0.05$, $\Delta(V - I) = 0.45 \pm 0.03$ in the case of Berkeley 32. Using the relation given by Carraro & Chiosi (1994), we derive log (age) = 9.8 ± 0.1 for the cluster. A slightly modified version of ΔV has been introduced by Janes & Phelps (1994) who used the luminosity difference between the RC and the inflection point between the turn-off region and the subgiant branch. We confirm their value of 2.4 for Berkeley 32. From their Fig. 1 one reads off the logarithm of age as 9.8-9.9, yielding an age of 6.3 - 8 Gyr. According to their Table 1, there are only a few clusters older than Berkeley 32, like NGC 6791, Berkeley 54, AM 2 and Cr 261. It is thus clear that Berkeley 32 belongs to the group of very old open clusters in our Galaxy.

5.3 Determination of the cluster parameters using theoretical isochrones

We have determined the colour excess, the distance modulus, and also the age of the cluster by fitting theoretical stellar evolutionary isochrones from the set of Bertelli et al. (1994) to our V, $(V - I)$ diagram. These isochrones are derived from stellar models computed with updated radiative opacities and include the effects of mass loss and convective core overshooting. The models trace the evolution from the zero-age main-sequence (ZAMS) to the central carbon ignition for massive stars and to the beginning of the thermally pulsing regime of the asymptotic giant branch phase for low and intermediate mass stars.

As most of the factors responsible for the colour spread in the MS will redden the stars (differential reddening, binaries, rotation, star spots), we have used the blue envelope of the MS in the CM diagram for the estimation of the cluster parameters. We fit the isochrones by eye taking into account the observational error. It turns out that the isochrone with log (age) = 9.8, $X = 0.7$, $Y = 0.28$ and $Z = 0.008$ fits best to the cluster locus, including the RC, and thus is in good agreement with the age estimated from the morphological parameters of the cluster

CMD. In order to also demonstrate upper limits of the effects of binaries in the CMD, the log (age) = 9.8 isochrone for the single stars has been brightened by 0.75 mag leaving the colour unchanged. A maximum reddening of $E(V-I) = 0.11$ (or $E(B-V) = 0.08$) mag can be applied to place the isochrone correctly on the cluster sequence observed in Fig. 4(B). Some stars above the turn-off point lie on the isochrones of binaries indicating the possibility of being indeed binary members of the cluster. The lower giant branch in the V, $(V-I)$ diagram appears marginally too blue, indicating that the cluster may have a slightly higher metallicity. However, a Z = 0.02 isochrone is definitely too metal-rich. Moreover, a solar metallicity would decrease the cluster reddening even further, while Kaluzny & Mazur (1991) quote a reddening of $E(B-V) = 0.16$ mag. However, such a high reddening is supported only by their V, $(U-V)$ diagram (see section 5.4).

It can also be seen that the theoretical location of the RC fits rather well with the observed one for Berkeley 32 unlike in some other old open star clusters (see Sagar & Griffiths 1999a). For example, it is too faint for NGC 6603 and too bright for NGC 7044.

The value of the apparent distance modulus derived from Fig. 4(B) is 12.8 mag. Here we adopt the reddening law of Rieke & Lebofsky (1985), who give $A_V/E(V-I) = 1.94$. With the extinction $A_V = 0.21$ mag, we get for Berkeley 32, a true distance modulus of 12.6 mag with an uncertainty of ~ 0.15 mag which includes errors in the photometric calibration, isochrone fitting and the reddening determination.

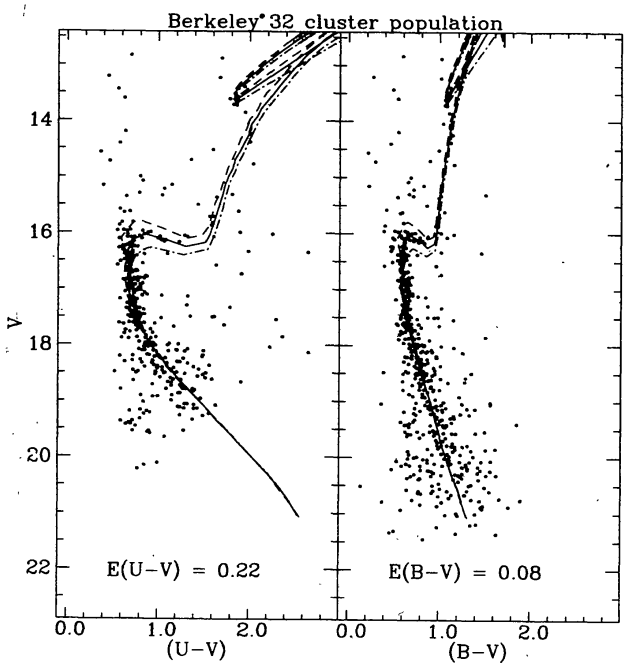

Figure 5. The V, $(U-V)$ and V, $(B-V)$ diagrams generated for the cluster population of Berkley 32 from the photometric data of Kaluzny & Mazur (1991). The Bertelli et al. (1994) isochrones of the same metallicity and ages, shifted by the same value of the apparent distance modulus as in Fig. 4(B) are shown. The best eye fits to the cluster sequence for the reddening values shown in the plot. The $E(U-V)$ value is not compatible with $E(B-V)$, including a problem with the U photometry.

5.4. Isochrone fitting to the UBV data of Kaluzny & Mazur (1991)

Fig. 5 shows the V, $(U-V)$ and V, $(B-V)$ diagrams generated from the Kaluzny & Mazur (1991) photometric data. Overplotted are the isochrones of Bertrelli et al. (1994), having the same ages, metallicity and helium abundance as we used for our V, $(V-I)$ diagram in Fig. 4(B). In order to fit the isochrone to the cluster sequence, we had to employ a reddening of $E(B-V)$ = -0.08 mag and $E(U-V) = 0.22$ mag in the V, $(B-V)$ and V, $(U-V)$ diagrams respectively. While for the reddening law of Rieke & Lebofsky (1985), the $E(B-V)$ value agrees well with our

Table 7. The age, metallicity ([*Fe/H*]), reddening ($E(B-V)$ and $E(V-I)$, true distance modulus ($(m-M)_O$), distance, galacto-centric distance (R_{GC}) (adopting galacto-centric distance of the Sun as 8 kpc) and z-distance for Berkeley 32.

Age	6.3 Gyr
[*Fe/H*]	-0.2 dex
$E(V-I)$; $E(B-V)$	0.11;0.08
$(m-M)_O$	12.60±0.1
Distance	3.3 kpc
R_{GC}	11.0 kpc
z	250 pc

$E(V-I)$ value ($E(V-I) / E(B-V) = 1.6$), the $E(U-V)$ is too large $E(U-V) / E(B-V) = 1.64$). On the orher hand, it is too small for $E(B-V) = 0.16$ mag, given by Kaluzny & Mazur (1991) and is thus not compatible with the reddening values derived from the V, $(V-I)$ and V, $(B-V)$ diagrams. This may suggest that the U-photometry is perhaps in error and we adopt $E(B-V) = 0.08$ mag as the value for the cluster reddening.

5.5 The cluster distance from the Red Clump

For a star cluster as old as Berkeley 32, an attractive method to determine its distance is using the location of the RC of intermediate-age helium core burning stars as a standard candle (e.g. Paczynski & Stanek 1998). The absolute I-magnitude of RC stars in the solar neighborhood has been calibrated by Hipparcos parallaxes, resulting in $M_I^0 = -0.23 \pm 0.03$. Code (1998) discusses the age and metallicity dependence of the RC-brightness and notes that for poulations older than 4-5 Gyr, the M_I^0 is independent of stellar mass, but still shows a metallicity dependence of the order $\delta M_I^0 = (0.21 \pm 0.07)$[*Fe/H*], where δM_I is the brightness difference between the RC in the solar neighborhood and the population under consideration. As the value is small for Berkeley 32, we neglect this correction here.

The RC in Berkeley 32 has $V = 13.67 \pm 0.03$ and $(V-I) = 1.16 \pm 0.03$, where the error is the uncertainty in the definition of the RC in the CMD. This yields $(m-M_I) = 12.74 \pm 0.08$ as the apparent distance modulus, if we include the photometric calibration uncertainty in the error. The extinction in I is determined by $A_I/E(V-I) = 0.93$ which is 0.10 for a value of $E(V-I) = 0.11$. If we assign an additional error of 0.05 to the extinction correction, we have $(m-M)_0 = 12.64 \pm 0.1$ as the value for true distance modulus. This agrees well with the value obtained

using isochrone fitting. In the following, we therefore adopt 12.6 ± 0.1 as the value for the distance modulus of the cluster. The present distance determination of 3.3 ± 0.2 kpc agrees very well with the value of 3.1 kpc given by Kaluzny & Mazur (1991). The cluster parameters derived by us are listed in Table 7.

5.6 Location of Berkeley 32 in the Galaxy

The cluster Berkeley 32 occupies an important position for understanding the variation of metallicity in the Galactic disk, as the issue of the existence of a metallicity gradient is not yet settled. According to Friel (1995), the metallicities of open clusters indicate a gradient of –0.09 dex/kpc. On the other hand, Twarog et al. (1997) argue that the open cluster system can be divided in 2 radial groups, with a very flat or even vanishing gradient in each group. Their mean metallicities differ by 0.3 dex and there is a discontinuity at a radial distance of 10 kpc. As the galactocentric distance of Berkeley 32 puts it just near this discontinuity, Berkeley 32 could help to decide between these two metallicity patterns in the Galactic disk. However, a more accurate determination of the metallicity than we are able to do, is required. Also, more clusters/objects either in the vicinity of Berkeley 32 or at similar galacto-centric distances need to be observed before the metallicity pattern can be unambiguously determined.

6. Mass function

The study of the mass function (MF) of Berkeley 32 is based on a pair of deep V and I CCD frames only. This is done for evaluating the data completeness accurately. Guided by the radial stellar density profile in Fig. 3, we selected stars located within a circle of 165 arcsec radius (surface area 23.76 square arcmin) around the cluster centre for the MF study. With the aim of detecting possible radial MF variations, the data completeness has first been evaluated in an inner and outer region separately, but it turned out to be the same within the errors. Besides, the small number statistics prevented us from a detailed study. We therefore determined the MF for the entire region without any subdivision.

To suppress the field star contamination as far as possible, we selected cluster main sequence stars by using the following boundaries in the V, $(V - I)$ diagram :

$$V > 8.91 + 9.45 \cdot (V - I) + 1.8 \cdot (V - I)^2$$

and

$$V < 11.52 + 12.64 \cdot (V - I) + 3.86 \cdot (V - I)^2$$

The field star contamination has been determined using the remaining chip area outside a radius of 265 arcsec (surface area 123.1 square arcmin) from the cluster centre. Table 8 lists the field and cluster counts derived in this way along with their completeness factors. The completeness factors have been determined by using artificial stars along the clusters main sequence and recovering them in the CMD, not in one filter, to be as realistic as possible. Table 8 also lists the numbers which are relevant for the MF determination. The transformation from apparent to absolute visual magnitude (M_V) has been done using the cluster parameters given in Table 7. The isochrone log(age) = 9.8 and $z = 0.008$ provides the following parametrization of mass (m) and M_V:

$$m = 1.665 - 0.186 \cdot M_V + 0.00698 \cdot M_V^2 .$$

The values of the normalised counts (N) are in stars/arcmin^2. They are corrected for completeness and field star contamination, and divided by the mass interval of the magnitude bin. The errors of the normalised counts result from error propagation. This may be incorrect from a puristic viewpoint, as they are no longer small compared to the counts. However, we do not use them any further beyond a qualitative demonstration that they are large.

A common description of the stellar mass spectrum is a power law $dN \propto m^{\alpha} dm$, where dN is the number of stars in the mass interval $m + dm$, and α is the slope of the MF. However,

Table 8. The V-magnitude of the bin center, the raw counts for cluster (N_C) and field regions (N_F), and the corresponding completeness factors f_C and f_F are listed. Absolute M_V and stellar mass (m) of the bin center, the mass interval (Δm) corresponding to the magnitude bin, the normalised counts (N) and their errors (δN) are also listed.

V	N_C	N_F	f_C	f_F	M_V	m	Δm	N	δN
16.25	41	53	1.00	1.00	3.40	1.113	0.0693	18.70	4.2
16.75	44	67	1.00	1.00	3.90	1.046	0.0658	19.88	4.6
17.25	47	86	1.00	1.00	4.40	0.982	0.0623	20.54	5.0
17.75	43	107	1.00	1.00	4.90	0.921	0.0588	16.00	5.1
18.25	50	135	0.95	1.00	5.40	0.864	0.0553	20.22	6.3
18.75	37	121	0.85	1.00	5.90	0.811	0.0518	16.39	6.3
19.25	35	127	0.80	0.93	6.40	0.761	0.0483	15.15	7.4
19.75	31	158	0.81	0.89	6.90	0.714	0.0449	3.76	7.4
20.25	37	154	0.80	0.90	7.40	0.671	0.0413	13.46	8.8
20.75	31	142	0.73	0.86	7.90	0.631	0.0379	11.73	8.9
21.25	24	116	0.60	0.70	8.40	0.595	0.0344	9.82	11.1

a uniform exponent is at best realised within limited mass intervals. The universality of the slope of the initial mass function (IMF) is still a matter of discussion (for a recent review see Scalo 1998), but studies of a large number of young clusters in the Milky Way and the Large Magellanic Clouds do not speak evidently against an universal IMF at least above 1 $M_{\odot}$ (e.g. Sagar et al. 1986; Sagar & Richtler 1991; Janes & Phelps 1994; Fischer et al. 1998; Sagar 2000), with α around –2.3. Below 1 $M_{\odot}$, the data for young open clusters are sparse and any secure statement on a possible universal IMF is not yet possible.

However, in the case of a very old cluster like Berkely 32, we might anyway not expect the IMF to be still realized. As a cluster evolves dynamically, low mass stars evaporate out of the cluster potential faster than high mass stars. In a cluster much older than its relaxation time, the dynamical effects therefore can change an originally rising IMF into a flat or even declining MF.

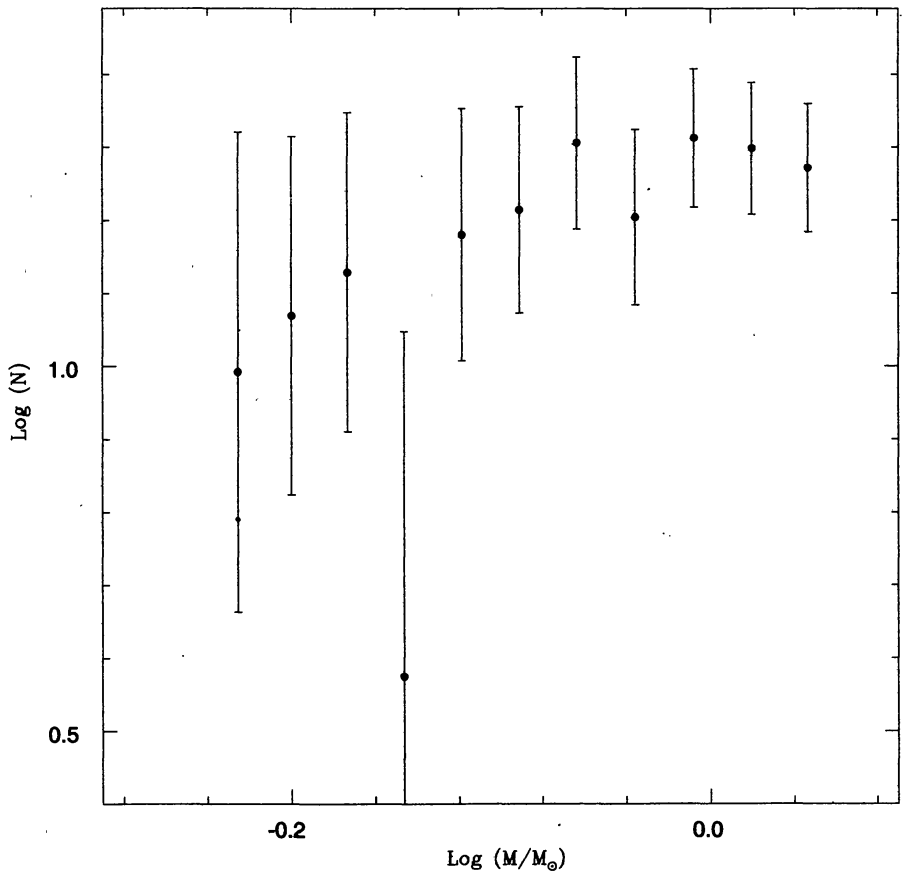

Figure 6. The mass function of Berkeley 32 between 0.6 and 1.1 $M_{\odot}$ as derived from the present data. Although the error bars are large, the mass function is clearly flatter than what has been found for young star clusters.

Fig. 6 shows the MF for Berkeley 32. The logarithm of mass is plotted against the logarithm of the normalised counts. Note that the binning in mass is also logarithmic. Although the errors are too large for any deeper analysis, it is apparent that the MF is much flatter than of most young clusters. A fit to a power-law indeed returns the value $\alpha = -0.5 \pm 0.3$ while we expect in this mass domain an exponent around –2 for young clusters (Richtler 1994). Here it must be remarked that we assumed single stars for the applied mass-luminosity relation of the isochrone. Sagar & Richtler (1991) discussed how the presence of binaries flattens a "true" IMF. But even if we find a large binary fraction in Berkeley 32, as the CMD suggests, their effect would by far not be sufficient to steepen the observed MF to the level as it is observed for young clusters.

This behaviour, in agreement with theoretical expectations, has been found for other old open clusters as well. For example, Francic (1989), among his sample of 8 open clusters, found the old objects NGC 752 (2.5 Gyr) and M67 (5 Gyr) to show even declining mass functions with $\alpha > 0$. Further well studied open clusters like NGC 6791 (Kaluzny & Rucinski 1995), NGC 188 (von Hippel & Sarajedini 1998), NGC 2243 (Bergbusch et al. 1991) also have flatter MFs. But one also can find old clusters with MF not distinguishable from a Salpeter mass function, e.g.,

mass spectrum of Berkeley 99 (age 3.2 Gyr) has $\alpha \sim -2.4$ (Sagar & Griffiths 1998b). This demonstrates that open clusters do have distinctly different dynamical histories, which may depend on their structure, total mass, location, orbit characteristics etc.

7. Summary

New V and I CCD photometry down to $V = 22$ mag is presented for about 3,200 stars in the region of the open cluster Berkeley 32. The present photometry serves as a data base for determining the cluster properties and to study the stellar mass function for the first time. The cluster's radial density profile is well represented by a King (1962) profile. By fitting of theoretical isochrones and using the location of the Red Clump, we confirm earlier results that it is indeed a very old open cluster (6.3 Gyr). Its metallicity is between $Z = 0.008$ and $Z = 0.02$, distance is 3.3 kpc and galacto-centric distance is 10.8 kpc. Clusters/objects with these characteristics can play a very valuable role to distinguish between the two models of the metallicity variation in the Galactic disk, advocated by Friel (1995) and Twarog et al. (1997) respectively. However, the case of Berkeley 32 is ambiguous. The parameters of Berkeley 32 are compatible with both a smooth Galactic metallicity gradient as well as with its membership of the cluster population of the inner domain of Twarog et al. (1997).

We also investigated the mass spectrum of Berkeley 32 in the mass range 0.6–1.1 $M_{\odot}$. A power-law fit returns $\alpha = -0.5 \pm 0.3$ for the slope of the MF, which is much flatter than the slopes found in young open clusters. Berkeley 32 shares this behaviour with other old open clusters which indicates an evaporation of low-mass cluster stars.

Acknowledgements

The suggestions/comments given by the referee Randy L. Phelps improved the presentation and readablity of the paper. RS gratefully acknowledges the support from the Alexander von Humboldt Foundation. TR wants to thank the U.P. State Observatory, Nainital, the Deutsche Forschungsgemeinschaft, and the Indian National Science Academy, for financial support and warm hospitality. Thanks to Klaas de Boer for going through the manuscript critically. The Open Cluster Data Base maintained by J.-C. Mermilliod has been used in the present work.

References

Bergbusch P.A., VandenBerg D.A., Infante L. 1991, AJ 101, 2102
Bertelli G., Bressan A., Chiosi C., Fagotto F., Nasi E., 1994, A&AS 106, 275
Carraro G., Chiosi C., 1994, A&A 287, 761
Cole A.A., 1998, ApJ 500, L137
Fischer P., Pryor C., Murray S., Mateo M., Murray S., Richtler T., 1998, AJ 115, 592
Francic S.P., 1989, AJ 98, 888
Friel E.D., 1995, ARA&A 33, 381
Iskudarjan S.G., 1960, Comm. Biur. 28, 46
Janes K.A., Phelps R.L., 1994, AJ 108, 1773
Kaluzny J., Rucinski S.M., 1995, A&AS 114, 1
Kaluzny J., Mazur B., 1991, Acta Astr. 41, 167
Kaluzny J., 1994, A&AS 108, 151

King I.R., 1962, AJ 67, 471

King I.R., 1964, Royal Obser. Bull. 82, 106

Landolt A., 1992 AJ 104, 340

Lyngå G., 1987. *Catalogue of Open Cluster Data*, 5th edition, 1/1 S7041, Centre de Donnees Stellaires, Strassbourg.

Paczynski B., Stanek K.Z., 1998, ApJ 494, L219

Pandey A.K., Durgapal A.K., Bhatt B.C., Mohan V., Mahra H.S., 1997, A&AS, 122, 111

Phelps R.L., Janes K.A., Montgomery K.A., 1994, AJ 107, 1079

Richtler T., 1994, A&A 257, 517

Rieke G.H., Lebofsky M.J., 1985, ApJ 288, 618

Sagar R., 2000, BASI 28, 55

Sagar R., Griffiths W.K., 1998a, MNRAS 299, 1

Sagar R., Griffiths W.K., 1998a, MNRAS 299, 777

Sagar R., Richtler T., 1991, A&A 250, 324

Sagar R., Piskunov A.E., Myakutin V.I., Joshi U.C., 1986, MNRAS 220, 383

Scalo J., 1998, in The Stellar Initial Mass Function (38th Herstmonceux Conf.), eds. G. Gilmore and D. Howell, ASP Conf.Ser. 142 (1998), p. 201

Scott J.E., Friel E.D., Janes K.A., 1995, AJ 109, 1706

Setteducati A.E., Weaver M.F., 1960 in Newly found stellar clusters, Radio Astronomy Laboratory, Berkeley

Stetson P.B., 1987, PASP 99, 191

Stetson P.B., 1992, in Astronomical Data Analysis Software and Systems I. Worrall D.M., Biemesderfer C. and Barnes J. (eds), ASP Conf. Ser. 25, p. 297

Twarog B., Ashman, K.M., Anthony-Twarog B.J., 1997, AJ 114, 2556

von Hippel T., Sarajedini A., 1998, AJ 116, 1789